

ADAPTIVE STEP SIZE ALGORITHMS FOR LANGEVIN DYNAMICS

A. LEROY*, B. LEIMKUHLER*, D. J. HIGHAM*, AND J. LATZ†

Abstract. We discuss the design of an invariant measure-preserving transformed dynamics for the numerical treatment of Langevin dynamics based on rescaling of time, with the goal of sampling from an invariant measure. Given an appropriate monitor function which characterizes the numerical difficulty of the problem as a function of the state of the system, this method allows the stepsizes to be reduced only when necessary, facilitating efficient recovery of long-time behavior. We study both the overdamped and underdamped Langevin dynamics. We investigate how an appropriate correction term that ensures preservation of the invariant measure should be incorporated into a numerical splitting scheme. Finally, we demonstrate the use of the technique in several model systems, including a Bayesian sampling problem with a steep prior.

Key words. adaptivity, stochastic differential equation, timestepping, equilibrium sampling

AMS subject classifications.
80-10, 65C30, 65C20

1. Introduction. Underdamped Langevin dynamics describes random movements of a particle in contact with an infinite energy reservoir [27, Sect. 2.2.3]. The position vector $x \in \Omega \subset \mathbb{R}^d$ and the momentum vector $p = M\dot{x}$, $p \in \mathbb{R}^d$, where M is a $d \times d$ positive definite mass matrix, describe the state of this particle throughout time. They satisfy the stochastic differential equations (SDEs):

$$(1.1) \quad \begin{cases} dx &= M^{-1}p dt, \\ dp &= -\nabla_x V(x) dt - \gamma p dt + \sqrt{\frac{2\gamma}{\beta}} M^{1/2} dW_t. \end{cases}$$

Here $V : \mathbb{R}^d \rightarrow \mathbb{R}$ is a potential function, $(W_t)_{t \geq 0}$ is a standard Brownian motion on \mathbb{R}^d , $\beta := (k_B T)^{-1}$ is a parameter representing the reciprocal temperature, where k_B denotes Boltzmann's constant, and T the absolute temperature. Throughout this work, $x, p, (W_t)_{t \geq 0}$ and other random objects are defined on a suitable probability space. In Langevin dynamics a system loses energy through friction, controlled by the parameter γ , and gains energy through stochastic fluctuations in such a way that the equilibrium state is described by the Gibbs-Boltzmann distribution with density $\rho_\beta(x, p) \propto \exp(-\beta H(x, p))$, where $H(x, p) = p^T M^{-1} p / 2 + V(x)$ is the energy of the system.

The Langevin system and its overdamped counterpart (see Section 2) have been widely used as sampling methods in many applications; notably in physics, chemistry, biology, social science, and machine learning ([1, 2, 16, 17, 22, 32]). In sampling, the potential V is chosen so that the SDE has a desired invariant measure, and hence samples consistent with this measure may be obtained by generating long Langevin dynamics paths. This integration is most often performed using a numerical method with fixed stepsize. When the trajectories of the system undergo sudden changes, or exhibit highly oscillatory modes, the stepsize must be small enough for the numerical method to remain stable. When the frequencies of the system vary as the system visits different regions, a fixed stepsize would need to be sufficiently small throughout the integration to reflect the most extreme scenario. These issues can lead to substantial

*School of Mathematics, The University of Edinburgh, UK. (alix.leroy@sms.ed.ac.uk, d.j.higham@ed.ac.uk, b.leimkuhler@ed.ac.uk)

†Department of Mathematics, The University of Manchester, UK. (jonas.latz@manchester.ac.uk)

computational overhead since the need for small stepsizes might be restricted to a region which is rarely visited. By varying the stepsize, adequate stability and accuracy can be maintained everywhere while computational costs are reduced.

This discussion motivates variable (adaptive) stepsize discretization, using smaller steps only where needed in the simulation; hence allowing for both higher accuracy and faster convergence toward the target distribution.

In this article, we introduce a time transformation for variable stepsize simulation of SDEs similarly to what is done in other time stepping [14] and meshing contexts [12, 15]. Our transformation uses knowledge of a monitor function to modify the dynamics in both the overdamped and underdamped cases. A correction term arising from the fluctuation-dissipation theorem is required to ensure the desired target distribution. The focus in this paper is on the calculation of averages with respect to the invariant probability measure defined by the Fokker-Planck equation associated to the SDE. We first present an overview of related work, and introduce a simple example to illustrate the efficiency of the transformed dynamics in Section 2. The main contributions of this work are as follows.

- In Section 3, a framework to design an efficient monitor function is presented, applicable even when little is known about the problem. We establish criteria on the function that are sufficient to maintain existence of the solution of the transformed dynamics.
- In Section 4, confirmation that the continuous overdamped transformed dynamics has the desired Gibbs distribution as a unique distribution when respecting the criteria outlined in Section 3.
- In Section 5, comparison of several numerical integrators to simulate the Gibbs distribution using the transformed underdamped dynamics.
- In Section 6 computational results for both overdamped and underdamped dynamics, in one and two dimensions, emphasizing the benefits and limitations of the method.

We give brief conclusions in Section 7.

There have been a number of approaches to designing variable stepsize strategies for strong (pathwise) approximation of SDEs [5, 8, 18, 36] with relatively little work addressing the issue of weak approximation [29, 43, 45, 46]. Works focusing on the approximation of invariant measures are even rarer, since the relevant analyses, even in the case of fixed stepsize, are fairly recent. The authors of [20] establish an adaptive algorithm preserving the ergodicity of the original SDEs and design an algorithm to control the drift term by halving or doubling the stepsize based on local error estimation and a user-provided tolerance. In [38], the authors focus on demonstrating the ergodicity of quasi-symplectic integrators, i.e., integrators that conserve a quantity of interest such as energy or momentum, and show that rejecting exploding trajectories does not affect ergodicity. Variable timestepping is certainly not the only approach to improve efficiency of Langevin simulations. For example, one may use an accept-reject step in conjunction with a Langevin proposal density [42] or Hamiltonian Monte Carlo [3, 6, 10] to handle the bias that may arise. In principle such techniques could be combined with variable stepsize to further improve efficiency.

Pre-conditioning methods offer an alternative approach for improving the exploration of the space in the Hamiltonian case; however these tend to be difficult to implement and computationally expensive [10, 33, 40]. Related problems in sampling are discussed in [7]; for example how to increase the spectral gap or minimise the asymptotic variance of the approximation [26, 28, 41]. Finally, similar approaches have been exploited in the context of machine learning and stochastic optimization,

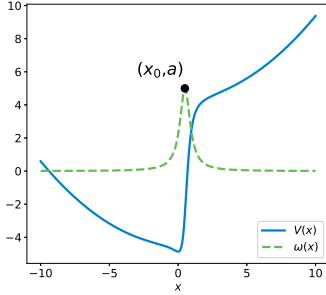
as in [30, 31], where adapting the learning rate is equivalent to varying the stepsize.

2. Motivating example. We consider an example with a modified harmonic potential, where the force applied to the molecule depends on the frequency and has the form

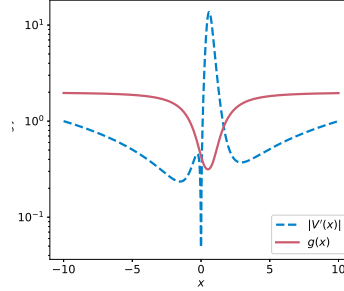
$$(2.1) \quad F(x) = -V'(x) = (\omega(x)^2 + c)x, \text{ with } \omega(x) = \frac{b}{\frac{b}{a} + (x - x_0)^2},$$

where $\omega : \mathbb{R} \rightarrow \mathbb{R}$ is the state dependent frequency. The potential V is defined by

$$(2.2) \quad V(x) = \frac{1}{2} \left(a^{\frac{3}{2}} b^{\frac{1}{2}} x_0 \arctan \left(\frac{a}{b} (x - x_0) \right) + \frac{ab(a(x - x_0)x_0 - b)}{a(x - x_0)^2 + b} + c(x - x_0)^2 + 2c(x - x_0)x_0 \right).$$



(a) The potential $V(x)$ and the function $\omega(x)$ with $a = 5$, $x_0 = 0.5$ and $b = 1$. A smaller value of b increases the values of ω around x_0 .



(b) The gradient V' and an example of monitor function g

FIG. 1. Plots of the potential, the absolute value of its derivative and an example of a monitor function g .

The Boltzmann-Gibbs distribution with density

$$(2.3) \quad \rho(x) = \frac{1}{Z} \exp(-\beta V(x)),$$

and normalising factor

$$(2.4) \quad Z = \int_{\mathbb{R}^d} \exp(-\beta V(x)) dx,$$

is the unique invariant distribution of the overdamped SDE

$$(2.5) \quad dx = -\nabla V(x) dt + \sqrt{2\beta^{-1}} dW$$

by [39, Proposition 4.2]. This result holds if the potential V is smooth and confining. The overdamped SDE (2.5) can be obtained from the underdamped system of SDEs (1.1) by asymptotic methods letting the mass go to zero or the friction to infinity (see [39, Sect. 6.5.1]). To obtain samples from the stationary distribution (2.3),

the standard approach is to discretize the overdamped SDE (2.5) using the Euler-Maruyama scheme

$$(2.6) \quad X_{n+1} = X_n - \nabla V(X_n)h + \sqrt{2\beta^{-1}h}\Delta W_n.$$

The stepsize h is fixed, $X_n \approx X(t = nh)$ and the increments ΔW_n are independent and $\Delta W_n \sim \mathcal{N}(0, 1)$. Figure 1(a) shows the values taken by the potential V , close to a square potential in most of the domain but steepening near x_0 . An example of an associated monitor function g is provided in Figure 1(b). This follows the variation of $\frac{1}{|V'(x)|}$ whilst being bounded by strictly positive values $m < M$, effectively decreasing the stepsize around the singularities, see equation (3.1) in Section 3. The parameters m and M define lower and upper bounds on the multiplicative factor of the stepsize.

In the next section, we describe a direct time-rescaled SDE which does not conserve the invariant measure, and then introduce the main focus of this paper in the invariant measure-preserving transformed SDE. Variable stepsize integration is implemented by defining a new time variable τ such that $\tilde{x}(\tau) = x(t(\tau))$. For a given monitor function $g(x) > 0; \forall x \in \mathbb{R}^d$, the time t is monotone in τ and defined by the relation

$$(2.7) \quad \frac{dt}{d\tau} = g(x(t(\tau))),$$

$$(2.8) \quad \frac{dW(t)}{dt} = \sqrt{g(\tilde{x})} \frac{d\tilde{W}(\tau)}{d\tau}.$$

Replacing the terms (2.7) in the overdamped SDE (2.5), the direct time-rescaled SDE is

$$(2.9) \quad d\tilde{x} = -\nabla V(\tilde{x})g(\tilde{x})d\tau + \sqrt{2\beta^{-1}g(\tilde{x})}d\tilde{W}(\tau),$$

with the Euler-Maruyama numerical scheme yielding

$$(2.10) \quad \tilde{X}_{n+1} = \tilde{X}_n - \nabla V(\tilde{X}_n)g(\tilde{X}_n)h + \sqrt{2\beta^{-1}g(\tilde{X}_n)h}\Delta W_n.$$

Using (2.6) and (2.10), we obtain samples using the discretized scheme and plot the histograms of the positions alongside the normalised stationary density (2.3) in Figure 2.

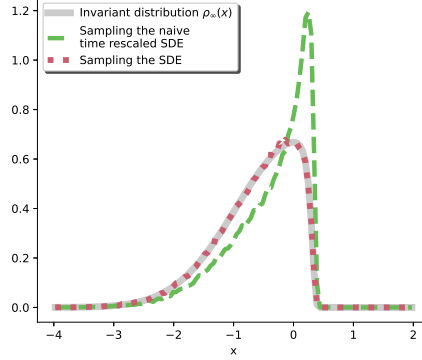


FIG. 2. Histograms of the invariant distribution and samples obtained using the Euler-Maruyama scheme applied (a) to the original SDE (2.5) and (b) to the direct time-rescaled SDE (2.9) after 50000 steps, with step of size $h = 0.001$, temperature $\beta^{-1} = 0.1$, and $n_s = 10^5$ samples. The function g is bounded by $M = 2$, $m = 0.001$. The parameters of the potential are set to $c = 0.1$, $b = 0.1$, $a = 10$ and $x_0 = 0.5$.

The numerical scheme applied to the direct time-rescaled SDE in Equation (2.10) does not yield samples that agree with the invariant distribution (2.3). In fact this has nothing to do with the discretization scheme itself; it is a consequence only of the time-rescaling of the dynamics. It can be understood by examining the adjoint operator of the infinitesimal generator associated with the direct time-rescaled equation (2.9):

$$(2.11) \quad \tilde{\mathcal{L}}^* \rho(t, \tilde{x}) = -\nabla \cdot (-\nabla V(\tilde{x})g(\tilde{x})\rho(t, \tilde{x}) + \beta^{-1}\nabla g(\tilde{x})\rho(t, \tilde{x})).$$

The invariant distribution (2.3) is a stationary density if it is in the kernel of the adjoint operator $\tilde{\mathcal{L}}^*$ [39, Sect. 4.1]. We see that

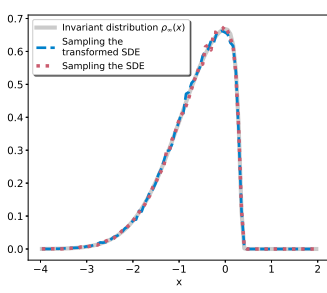
$$(2.12) \quad \tilde{\mathcal{L}}^* \rho(\tilde{x}) = -\beta \nabla V(\tilde{x})\rho(\tilde{x}),$$

noting that the invariant distribution (2.3) respects $\nabla \rho(x) = -\beta \nabla V(x)\rho(x)$ by the chain rule. As $\tilde{\mathcal{L}}^* \rho(\tilde{x}) \neq 0$, the probability distribution (2.3) is not in the kernel of the adjoint operator $\tilde{\mathcal{L}}^*$. This motivates a correction that leads to an invariant measure-preserving transformed SDE that retains the stationary distribution of the original SDE

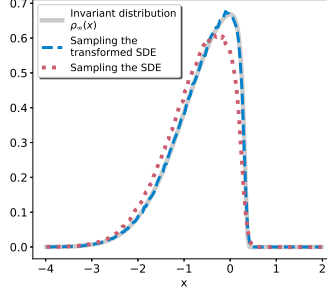
$$(2.13) \quad dx = -g(x)\nabla V(x)dt + \beta^{-1}\nabla g(x)dt + \sqrt{2\beta^{-1}g(x)}dW.$$

From now, we will only consider this invariant measure-preserving transformed SDE using x and t variables, which we refer to as IP transformed SDE. The associated Euler-Maruyama scheme is

$$(2.14) \quad X_{n+1} = X_n - \nabla V(X_n)g(X_n)h + \beta^{-1}\nabla g(X_n)dt + \sqrt{2\beta^{-1}g(X_n)h}\Delta W_n.$$



(a) Samples obtained with step of size $h = 0.001$ to reach the final time $T = 50$.



(b) Samples obtained with step of size $h = 0.05$ to reach the final time $T = 70$.

FIG. 3. Histograms of the invariant distribution and samples from Euler-Maruyama scheme applied to the original SDE (2.5) and to the IP transformed SDE (2.13) with $n_s = 10^5$ samples, using the function g plotted in Figure 1(b) with $M = 2$, $m = 0.001$, a temperature of size $\beta^{-1} = 0.1$. The parameters of the potential are set to $c = 0.1$, $b = 0.1$, $a = 10$ and $x_0 = 0.5$.

As shown in Figure 3(a), the discretized scheme (2.14) allows us to sample from the invariant distribution ρ_{eq} . It not only provides samples from the desired distribution, but moreover remains accurate for larger stepsizes, as seen in Figure 3(b). While the processes (2.5) and (2.13) are different, the values taken by $g(X_n)$ can be used as a proxy to the computational effort provided by the invariant-preserving transformed dynamics. We note that to yield the sample in Figure 3(b), the mean value of the monitor function g over all samples and iterations is 1.513, which suggests that simulating the SDE (2.13) is computationally more efficient, i.e. a timestep of size 1.513 would yield a similar accuracy.

We could alternatively obtain samples from the invariant measure by using the direct time-rescaled scheme (2.10) as follows: first, for a fixed value of T we ensure that the sum of the rescaled timesteps $g(\tilde{X}_n)h$ taken along the trajectory reach the same final time T , rather than fixing the number of steps, where interpolation is needed to obtain the values of the sample at the precise time T . Using this as the finite time sampling procedure, we then let $T \rightarrow \infty$.

3. Design of monitor function. A smart choice of the monitor function g decreases the fictive stepsize in regions of high solution change and increases it elsewhere. In this section, we give some intuition regarding the design of a “good” monitor function, as well as criteria that guarantee that the well-posedness of the SDE.

3.1. Stepsize bounds. In the example with the potential (2.2), the function g decreases the stepsize where the potential is steep and increases it elsewhere. This allows us to gain accuracy, as it encourages trajectories to approach the equilibrium values in the numerical integration. Different designs of the monitor function g are available.

The simplest choice (if not the most practical) is to base the monitor function on $G(x) = \|V'(x)\|$ ¹. But simply choosing $g(x) = 1/G(x)$ is unreliable since the forces may vanish entirely or become very large, causing the stepsize either to grow precipitously or decay to zero. Instead, it is desirable to introduce a heuristic, as in

¹The notation $\|\cdot\|$ stands for the 2-norm.

[14], which controls the adapted stepsize to lie within a fixed range.

Define a smooth, monotone function $\psi : \mathbb{R}_+ \rightarrow [m, M]$, for $m < M$ such that:

$$\lim_{u \rightarrow \infty} \psi(u) = m, \quad \lim_{u \rightarrow 0} \psi(u) = M.$$

For this choice the composite function $g(x) = \psi(1/G(x))$ has a defined range and has the property that $g(x)$ is minimized in the limit of large $G(x)$, and is maximal when $G(x) \approx 0$. We used a similar choice to the one suggested in [14],

$$(3.1) \quad \psi(x) = \left(\frac{\sqrt{1 + m^2 r x^{2\alpha}}}{1/M \sqrt{1 + m^2 r x^{2\alpha}} + \sqrt{r x^{2\alpha}}} \right)$$

where we added the dependence on the power $\alpha \in \mathbb{N}_+$ and the parameter $r \in \mathbb{R}_+$, which has more rapid decay for larger r , see Figure 4. The latter reaches $\frac{mM}{m+M}$ at $u = 0$, but if $m \ll M$, this difference is inconsequential.

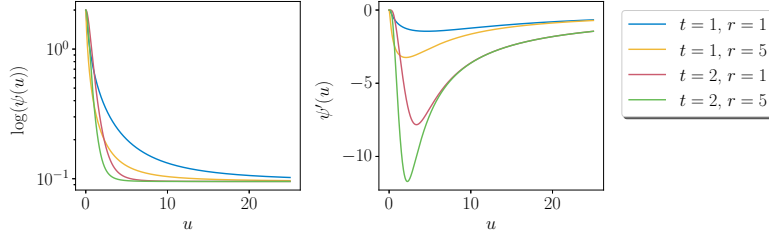


FIG. 4. Comparison of the monitor function for different values of the parameter r and t .

By choosing the coefficients m, M and the fictive (transformed time) stepsize h appropriately, we can restrict the effective stepsize to any desired range. Referring to the example in Section 2, we define $g_1(x) = \psi(V'(x))$, $g_2(x) = \psi(\omega^2(x))$ and $g_3(x) = \psi(\omega(x))$, as shown in Figure 5.

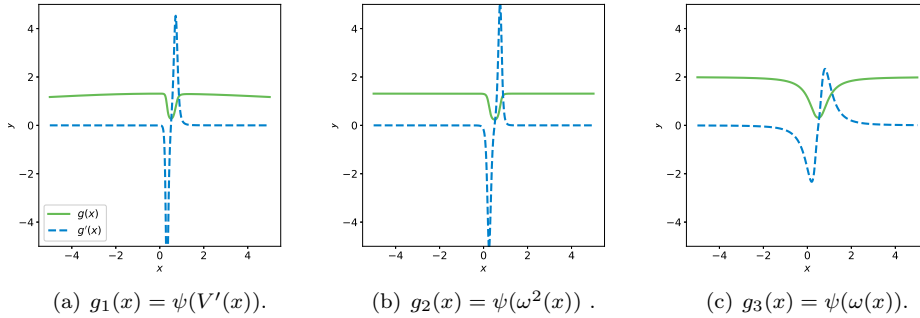


FIG. 5. Different designs of the function g , and the corresponding function g' .

In Figure 5, we plot the functions g_1 , g_2 and g_3 , respectively from left to right. We observed that the numerical integration remained stable for larger stepsize with

the function g_3 . This is due to the smaller values taken by g'_3 , allowing us to obtain comparable results with a large range of stepsizes and providing informative accuracy curves (presented in Section 6). More rapid changes of the function g will induce higher values of ∇g , which means that smaller steps will be required for the numerical integration. This highlights an important balance one needs to strike when designing g . A highly adaptive monitor function g can provide better efficiency but will induce a large correction term that might impair the stability of the SDE. Intuitively, it may be argued that we are attempting to ease the integration of the SDE with drift terms having a large Lipschitz constant by introducing a taming multiplicative factor in the form of a monitor function.

With a good design of monitor function, the numerical integrators reach their asymptotic state with lower computational effort, or, equivalently, for a larger mean stepsize. With the original systems (1.1) and (2.5), larger stepsizes do not allow the numerical integration to weakly approach the target distribution. In the general non-scalar case, without detailed knowledge of the problem, a simple heuristic monitor function could be taken to be $\psi(\|\nabla V(x)\|)$, but there are often better choices. For example, if the computation of the potential is very expensive, one may use a simplified, more computable measure of its magnitude. An example arises in N -body simulation where interactions with distant bodies contribute little to the overall potential or gradient norm; these long-range terms can be neglected in calculating the monitor function, saving considerable computation. Other examples arise in Bayesian parameter inference when the prior distribution is steeply confined but the model likelihood is smooth.

3.2. Well-posedness of the IP transformed SDE. From [49, Theorem 5.2.1] an SDE with drift term $b : [0, \infty[\times \mathbb{R}^d \rightarrow \mathbb{R}^d$ and diffusion $\sigma : [0, \infty[\times \mathbb{R}^d \rightarrow \mathbb{R}^d$ has a unique solution x that is continuous with respect to time under global Lipschitz conditions

$$(3.2a) \quad \|b(t, x) - b(t, y)\| \leq C_1 \|x - y\|; \quad x, y \in \mathbb{R}^d$$

$$(3.2b) \quad \|\sigma(t, x) - \sigma(t, y)\| \leq C_2 \|x - y\|; \quad x, y \in \mathbb{R}^d.$$

for some constant C_1, C_2 . We now derive criteria that may be imposed on the monitor function to ensure that these conditions are satisfied for the IP transformed SDE.

We make the following assumptions on the potential

ASSUMPTION 1. *The potential V is smooth and confining, hence the Gibbs distribution (2.3) is the unique invariant distribution of the SDE (2.5).*

ASSUMPTION 2. *The potential is a measurable function satisfying*

$$(3.3) \quad \|\nabla V(y) - \nabla V(x)\| \leq D \|x - y\|; \quad x, y \in \mathbb{R}^d$$

for some constant D , which implies

$$(3.4) \quad \|\nabla V(x)\| \leq C(1 + \|x\|); \quad x \in \mathbb{R}^d$$

for some constant C .

The IP transformed SDE (2.13) has a drift term $\tilde{b}(x) = -\nabla V(x)g(x) + \beta^{-1}\nabla g(x)$ and a diffusion term $\tilde{\sigma}(x) = \sqrt{2\beta^{-1}g(x)}$. The monitor function g is assumed to be differentiable, and we enforce a global Lipschitz condition on this function and its gradient.

CRITERION 1. *There exists a constant $C_1 > 0$ such that*

$$(3.5) \quad |g(x) - g(y)| \leq C_1 \|x - y\|; \quad x, y \in \mathbb{R}^d.$$

CRITERION 2. *The function ∇g exists and there exists a constant $C_2 > 0$ such that*

$$(3.6) \quad \|\nabla g(x) - \nabla g(y)\| \leq C_2 \|x - y\|; \quad x, y \in \mathbb{R}^d.$$

In practice, the function g is built to re-scale the value of the stepsize and, thus, is bounded.

CRITERION 3. *The function $g : \mathbb{R}^d \rightarrow \mathbb{R}$ is such that there exist two strictly positive constants M_1, m_1 , with $m_1 < M_1$, such that*

$$(3.7) \quad M_1 > g(x) > m_1; \quad x \in \mathbb{R}^d.$$

We note that Criterion 1 implies that the drift term $\sqrt{2\beta^{-1}g}$ is Lipschitz as \sqrt{x} is Lipschitz on $\{x \in \mathbb{R} | x > m_1\}$ and Criterion 3 ensures that $g(x) > m_1; x \in \mathbb{R}^d$. Thus, the diffusion term $\tilde{\sigma}(x) = \sqrt{2\beta^{-1}g(x)}$ satisfies (3.2b). Finally, we require that the product $\nabla V g$ is Lipschitz. The function g is smooth and bounded, and the potential is also smooth and confining. The function g may be defined to be constant outside a suitable ball, so our final criterion holds by design.

CRITERION 4. *There exists a constant $C_3 > 0$ such that*

$$(3.8) \quad \|\nabla V(x)g(x) - \nabla V(y)g(y)\| \leq C_3 \|x - y\|; \quad x, y \in \mathbb{R}^d.$$

Then, by the triangle inequality, the Criteria 1 and 4 ensure that the drift term $\tilde{b}(x) = -\nabla V(x)g(x) + \beta^{-1}\nabla g(x)$ respects (3.2a). The desired proposition follows.

PROPOSITION 3.1. *If $b(x) \equiv -\nabla V(x)$ in the SDE (2.5) satisfies condition (3.2a) then, under Assumptions 1 and 2 and Criteria 1 - 4, the IP transformed SDE (2.13) satisfies condition (3.2a) and (3.2b) and hence has a unique solution that is continuous with respect to time.*

4. Invariant distribution and geometric ergodicity. In Section 2, our proposed correction in (2.13) is necessary to ensure stationarity with respect to the correct distribution and in Section 3.2, we showed there exist a unique time continuous process for equation (2.13). In the following section, using uniform ellipticity of the Fokker-Planck equation, we show that the Gibbs distribution is the unique invariant distribution to equation (2.13). Additionally, we introduce the transformed version of the underdamped Langevin equations (1.1) and provide results in this case which correspond to those obtained for overdamped systems. The underdamped system is, in principle, more challenging but we outline a simpler approach here that gets around invoking such a complicated analysis.

4.1. The overdamped Langevin dynamics. We follow Theorem 4.1 [39, p 89], which applies to the time homogeneous process x in equation (2.5) where the diffusion matrix is the product of the diffusion term $\sigma(x) = \sqrt{2\tau}$, i.e $\Sigma(x) = \sigma(x)\sigma(x)^T : \mathbb{R}^{d \times d} \rightarrow \mathbb{R}^{d \times d}$, with an initial condition X_0 with probability density function $\rho_0(x)$. The solution $u(x, t) \in C^{2,1}(\mathbb{R}^d \times \mathbb{R}^+)$ is the solution to an initial value problem with a uniform elliptic backward Kolmogorov equation of the form

$$\frac{\partial u}{\partial t} = \frac{1}{2}\Sigma(x) : D^2 u + \tilde{b}(x) \cdot \nabla u + c(x)u$$

². If we have uniform ellipticity on the diffusion, there exists a constant $\alpha > 0$ such that

$$(4.1) \quad \langle \xi, \Sigma(x)\xi \rangle \geq \alpha \|\xi\|^2, \quad \forall \xi \in \mathbb{R}^d,$$

uniformly in $x \in \mathbb{R}^d$ which is trivial for (2.5). If uniform ellipticity holds and if the coefficients $\tilde{b}(x) = \nabla V(x) + \nabla \cdot \Sigma(x)$ and $c(x) = \nabla \cdot \nabla V(x) + \frac{1}{2} \nabla \cdot (\nabla \cdot \Sigma)(x)$ are smooth and satisfy the growth conditions

$$(4.2a) \quad \|\Sigma(x)\| \leq B_1,$$

$$(4.2b) \quad \|\tilde{b}(x)\| \leq B_2(1 + \|x\|),$$

$$(4.2c) \quad \|c(x)\| \leq B_3(1 + \|x\|^2),$$

then, there exists a unique solution to the Cauchy problem for the Fokker Planck equation. For equation (2.5), conditions (4.2a) follows from the constant diffusion term and (4.2b) is equivalent to the linear growth assumption in equation (3.4). The following assumption is made on the potential to ensure (4.2c).

ASSUMPTION 3. *There exist a constant $C_4 > 0$ such that*

$$(4.3) \quad \left\| \sum_{i=1}^d \partial_{x_i}^2 V(x) \right\| \leq C_4(1 + \|x\|^2); x \in \mathbb{R}^d.$$

We show that theorem 4.1 holds for the transformed equation (2.13), provided two additional criterions on the monitor function.

CRITERION 5. *The function $\nabla g : \mathbb{R}^d \rightarrow \mathbb{R}^d$ is such that there exist two strictly positive constants M_2, M_3 such that for all x*

$$(4.4) \quad M_2 > \|\nabla g(x)\|; \quad x \in \mathbb{R}^d.$$

and for $j = 1, \dots, d$, we have

$$(4.5) \quad M_3 > |\partial_j g(x)|; \quad x \in \mathbb{R}^d.$$

and

CRITERION 6. *The function $g : \mathbb{R}^d \rightarrow \mathbb{R}^d$ is twice differentiable and has bounded second derivative. For $i, j = 1, \dots, d$, we have*

$$(4.6) \quad M_4 > |\partial_{x_i}^2 g(x)|; \quad x \in \mathbb{R}^d.$$

we can

THEOREM 4.1. *If the SDE (2.5) satisfies the Assumptions 1 to 3 and provided that the monitor function follows Criteria 5 to 6, the IP transformed SDE (2.13)*

$$dx = -g(x)\nabla V(x)dt + \beta^{-1}\nabla g(x)dt + \sqrt{2\beta^{-1}g(x)}dW.$$

has the unique invariant distribution ρ_{eq} , as given in (2.3).

²Note that $\frac{1}{2}\Sigma(x) : D^2 u = \frac{1}{2} \sum_{i=1}^d \sum_{j=1}^d \Sigma_{ij}(x) \partial_{x_i}^2 \partial_{x_j}^2 u$

Proof. Firstly, we demonstrate that the distribution (2.3) is invariant with respect to the SDE (2.13). It can be seen by examining the adjoint operator of the infinitesimal generator associated with equation (2.13)

$$\mathcal{L}^* \rho(t, x) = -\nabla \cdot (-\nabla V(x)g(x) + \beta^{-1}\nabla g(x)\rho(t, x) + \beta^{-1}\nabla g(x)\rho(t, x)).$$

The invariant distribution (2.3) is a stationary density if it is in the kernel of the adjoint operator \mathcal{L}^* . We have

$$\mathcal{L}^* \rho_{\text{eq}} = -\nabla \cdot (-\nabla V(x)g(x) + \beta^{-1}\nabla g(x)) \rho_{\text{eq}} + \beta^{-1}\nabla \cdot (\nabla g(x)\rho_{\text{eq}} + g(x)\nabla \rho_{\text{eq}}),$$

and we use consecutively the chain rule and distribute the gradient to expand the last term, and since g is scalar valued, we have

$$\begin{aligned} \mathcal{L}^* \rho(t, x) &= \nabla \cdot g(x)\nabla V(x)\rho(t, x) - \nabla \cdot g(x)\nabla V(x)\rho(t, x) \\ &\quad - \beta^{-1}\nabla \cdot \nabla g(x)\rho(t, x) + \beta^{-1}\nabla \cdot \nabla g(x)\rho(t, x) \\ &= 0, \end{aligned}$$

and the probability distribution (2.3) is in the kernel of the adjoint operator $\tilde{\mathcal{L}}^*$ and is an invariant distribution of the SDE (2.13). Secondly, we prove uniqueness of the solution by showing that conditions (4.1) and (4.2) hold for the transformed dynamic (2.13). Firstly, the diffusion matrix $\tilde{\Sigma}(x) = 2\beta^{-1}g^2(x)\mathbf{I}$ of the SDE (2.13) respects (4.1) and (4.2a) by Criterion 3. We note that for the IP transformed SDE (2.13), the condition (4.2b) is applied on $\|\hat{b}(x)\| = \|\nabla V(x)g(x) + \beta^{-1}\nabla g(x) + \nabla \cdot \sqrt{2\beta^{-1}g(x)}\mathbf{I}\|$. Using the triangle inequality and computing the divergence of the last term

$$\|\hat{b}(x)\| \leq \|\nabla V(x)g(x)\| + \|\beta^{-1}\nabla g(x)\| + \frac{\sqrt{2\beta^{-1}}}{2} \left\| \frac{\nabla g(x)}{\sqrt{g(x)}} \right\|,$$

noting that $\nabla \cdot g(x)\mathbf{I} = \nabla g(x)$ and $\nabla \cdot (\sqrt{\beta^{-1}2g(x)}\mathbf{I}) = \frac{\sqrt{2\beta^{-1}}}{2\sqrt{g(x)}}\nabla g(x)$. We can now use the Cauchy–Schwarz inequality on the first and last term, while bounding the second term using Criterion 5.

$$\|\hat{b}(x)\| \leq \|\nabla V(x)\| |g(x)| + \beta^{-1}M_2 + \frac{\sqrt{2\beta^{-1}}}{2} \left\| \frac{1}{\sqrt{g(x)}} \right\| M_2$$

The first term is bounded by linear growth through Assumption 2, and the monitor function is bounded by criteria 3. The last term is bounded by a constant through Criterion 3 and 5, which implies that (4.2b) holds. Finally, the last condition (4.2c) for $\|c(x)\| \leq M(1 + \|x\|^2)$ with $\|c(x)\| = \|\nabla \cdot (b(x)g(x) + \beta^{-1}\nabla g(x)) + \frac{1}{2}\nabla \cdot \nabla \cdot \sqrt{2\beta^{-1}g(x)}\mathbf{I}\|$. Using the triangle inequality, each term can be bounded separately, we have

$$\begin{aligned} \|c(x)\| &\leq \left| \sum_{i=1}^d (-\partial_{x_i}^2 V(x)) g(x) + b(x)\partial_{x_i} g(x) \right| + \beta^{-1} \left| \sum_{i=1}^d \partial_{x_i}^2 g(x) \right| \\ &\quad + \frac{\sqrt{2\beta^{-1}}}{2} \left| \sum_{i=1}^d \left(\frac{\partial_{x_i}^2 g(x)}{\sqrt{g(x)}} - \frac{1}{2} \frac{(\partial_{x_i} g(x))^2}{\sqrt{g(x)}^3} \right) \right|. \end{aligned}$$

The first term is bounded by respectively the linear and quadratic growth assumptions on the potential and its divergence (i.e Assumption 2 and 3) and criterion 3 and 5 on the monitor function. The second term is bounded by a constant through Criteria 5. The third term is bounded by constant through the criterion 3, 5 and 6. Thus, we have that condition (4.2c) holds as

$$\|c(x)\| \leq M(1 + \|x\|^2)$$

in the transformed case. Thus all conditions are respected and the invariant distribution is unique by theorem 4.1. \square

4.2. Underdamped Langevin dynamic. The underdamped Langevin dynamics (1.1), under Assumption 1, has the unique invariant distribution

$$(4.7) \quad \rho_{\text{eq}}^{\text{under}}(x, p) = \frac{1}{Z} \exp(-\beta H(x, p)),$$

where H is the Hamiltonian $H(x, p) = |p|^2/2 + V(x)$ and the normalizing factor Z is

$$(4.8) \quad Z = \int_{\mathbb{R}^{2d}} \exp(-\beta H(x, p)) dx dp,$$

by [39, Prop. 6.1]. We have the following relationships for the invariant distribution

$$(4.9a) \quad \nabla_x \rho_{\text{eq}}^{\text{under}} = -\beta \nabla_x V(x) \rho_{\text{eq}}^{\text{under}},$$

$$(4.9b) \quad \nabla_p \rho_{\text{eq}}^{\text{under}} = -\beta p \rho_{\text{eq}}^{\text{under}}.$$

We introduce a time-rescaling together with a modification of the force which preserves the invariant measure to yield the IP transformed underdamped dynamics.

THEOREM 4.2. *When Assumptions 1 and 2 and Criteria 1 to 4 hold, the system of SDEs*

$$(4.10) \quad \begin{cases} dx &= g(x) p dt, \\ dp &= -g(x) \nabla_x V(x) dt + \beta^{-1} \nabla_x g(x) dt - \gamma g(x) p dt + \sqrt{2\gamma\beta^{-1}g(x)} dW_t \end{cases}$$

has the invariant distribution (4.7)

$$(4.11) \quad \rho_{\text{eq}}^{\text{under}}(x, p) = \frac{1}{Z} \exp(-\beta H(x, p)),$$

with normalizing constant (4.8)

$$(4.12) \quad Z = \int_{\mathbb{R}^{2d}} \exp(-\beta H(x, p)) dx dp$$

Proof. To show that the equation (4.7) is a solution to the system (4.10), we introduce the initial value problem for the forward Kolmogorov equation associated to the system (4.10) with transition density $u(t, x, p) \in C^{2,1}(\mathbb{R}^+ \times \mathbb{R}^d \times \mathbb{R}^d)$. This is given by

$$(4.13) \quad \begin{aligned} \mathcal{L}^* u &= - \begin{pmatrix} \nabla_x \\ \nabla_p \end{pmatrix} \cdot \begin{pmatrix} pg(x) \\ -(\nabla_x V(x))g(x) + \beta^{-1} \nabla_x g(x) - \gamma g(x)p \end{pmatrix} u \\ &\quad + \frac{1}{2} \begin{pmatrix} \nabla_x \\ \nabla_p \end{pmatrix} \cdot \begin{pmatrix} \nabla_x \\ \nabla_p \end{pmatrix} \cdot \left(\begin{pmatrix} 0 & 0 \\ 0 & \sqrt{2g(x)\frac{\gamma}{\beta}} \end{pmatrix} \begin{pmatrix} 0 & 0 \\ 0 & \sqrt{2g(x)\frac{\gamma}{\beta}} \end{pmatrix}^T u \right) \end{aligned}$$

which yields

$$(4.14) \quad \begin{aligned} \mathcal{L}^* u = & -\nabla_x(g(x)p)u - \nabla_p \left[-g(x)(\nabla_x V(x)) + \beta^{-1}\nabla_x g(x) - \gamma g(x)p \right] u \\ & + \gamma\beta^{-1}g(x)\Delta_p u. \end{aligned}$$

Replacing u by $\rho_{\text{eq}}^{\text{under}}$ and using the (4.9b), the last two terms cancel as the configuration dependence of $g(x)$ plays no role, i.e. it corresponds to an Ornstein-Uhlenbeck SDE which automatically preserves $\rho_{\text{eq}}^{\text{under}} - \Delta_p(\gamma g(x)p)\rho_{\text{eq}}^{\text{under}} = \gamma\beta^{-1}g(x)\Delta_p\rho_{\text{eq}}^{\text{under}}$. Using the product rule in the first term and (4.9a), as well as (4.9b) on the second and third term, we are left with

$$\begin{aligned} \mathcal{L}^* \rho_{\text{eq}} = & -p(\nabla_x g(x))\rho_{\text{eq}} + \beta p g(x)\nabla_x V(x)\rho_{\text{eq}} + p(\nabla_x g(x))\rho_{\text{eq}} \\ & - \beta p g(x)\nabla_x V(x)\rho_{\text{eq}} \end{aligned}$$

implying that $\mathcal{L}^* \rho_{\text{eq}} = 0$. \square

Since the noise only appears in the momentum equation, the second order term depends only on the momentum p , and we can not use a similar reasoning for the system (4.10), but hypoellipticity of the operator can be shown using the Hörmander condition to show uniqueness of the solution [13]. A discussion can be found in [39, Section 6.1].

An alternative intuitive reasoning resides in taking the first moments with respect to $\rho_{\text{eq}}^{\text{under}}$ of the process X_t associated to the system (4.10). The expression $\lim_{t^* \rightarrow \infty} \frac{1}{t^*} \int_0^{t^*} f(X_t) dt$ under the change of variable $dt = g^{-1}(X_\tau) d\tau$ is

$$(4.15) \quad \lim_{\tau(t^*) \rightarrow \infty} \frac{\frac{1}{\tau(t^*)} \int_0^{\tau(t^*)} f(X_\tau) g^{-1}(X_\tau) d\rho_{\text{eq}}^{\text{under}}(\tau)}{\frac{1}{\tau(t^*)} \int_0^{\tau(t^*)} g^{-1}(X_\tau) d\rho_{\text{eq}}^{\text{under}}(\tau)}.$$

Under a similar change of variable $d\tau = g(X_\tau) dt$, it is easy to show that the system (4.10) becomes

$$\begin{cases} dy &= p d\tau, \\ dp &= (-\nabla_x V(x) + \beta^{-1}\nabla_x \log(g(x))) d\tau - \gamma p d\tau + \sqrt{2\gamma\beta^{-1}} dW, \end{cases}$$

with invariant distribution

$$\hat{\rho}_{\text{eq}}^{\text{under}} = \hat{Z} \exp \left(-\beta V(x) + \log g(x) + \frac{\|p\|^2}{2} \right).$$

From [35], condition 3.1 states that for such an underdamped system 4.2, $F(x) = (V(x) - \beta^{-1} \log(g(x)))$ is such that $F(x) \geq 0$, $\forall x \in \mathbb{R}^d$, and that there exists an $\alpha > 0$ and a $\beta \in (0, 1)$ such that

$$(4.16) \quad \frac{1}{2} \langle F(x), x \rangle \geq \beta F(x) + \gamma^2 \frac{\beta(2-\beta)}{8(1-\beta)} \|x\|^2 - \alpha$$

which applies if F grows at infinity as $\|x\|^{2l}$, where l is some positive integer. This condition is true by Assumption 1 and by $\log(g(x))$ being bounded by Criterion 3. Theorem 3.2 guarantees uniqueness of the invariant measure and geometric ergodicity, and the expression (4.15) can be written as

$$\frac{\int_{\Omega} \exp(-\beta V(x) + \log g(x)) f(x) g^{-1}(x) d\rho_{\text{eq}}^{\text{under}}(x)}{\int_{\Omega} \exp(-\beta V(x) + \log g(x)) g^{-1}(x) d\rho_{\text{eq}}^{\text{under}}(x)}.$$

Under the usual change of variable, we recover the space average of the system 4.10

$$\frac{\int_{\Omega} \exp(-\beta V(x)) f(x) d\rho_{\text{eq}}^{\text{under}}(x)}{\int_{\Omega} \exp(-\beta V(x)) d\rho_{\text{eq}}^{\text{under}}(x)}$$

using $\exp(\log g(x)) g^{-1}(x) = 1$. This implies ergodicity of the continuous process (4.10).

$$\lim_{t^* \rightarrow \infty} \frac{1}{t} \int_0^{t^*} f(X_t) d\rho_{\text{eq}}^{\text{under}}(t) = \int_{\Omega} \exp(-\beta V(x)) f(x) d\rho_{\text{eq}}^{\text{under}}(x)$$

which shows the ergodicity of the continuous process (4.10).

5. Numerical integrators. Having shown that the continuous processes have the unique Gibbs distribution as invariant distribution, we turn our focus to the design numerical methods for (2.13) and (4.10). Regarding the overdamped system, a sufficient condition to guarantee that the numerical approximation of the long term behaviour of the stochastic differential equation converges to the invariant distribution is provided by [34, Theorem 5.1, 5.2, 5.3]. For the underdamped system (1.1), a simple and popular approach to numerical timestepping integration is based on splitting schemes [4, 37, 44], which break the equations into separate parts which can be solved independently. Following the approach of [21, 23], we use splitting schemes which are built from the building blocks A, B and O as illustrated below:

$$(5.1) \quad d \begin{pmatrix} x \\ p \end{pmatrix} = \underbrace{\begin{pmatrix} p \\ 0 \end{pmatrix} dt}_{\text{A}} + \underbrace{\begin{pmatrix} 0 \\ -\nabla V(X) \end{pmatrix} dt}_{\text{B}} + \underbrace{\begin{pmatrix} 0 \\ -\gamma p dt + \sqrt{2\beta^{-1}} dW_t \end{pmatrix}}_{\text{O}}$$

Letter sequences denote numerical methods so for example the operator associated to the method ABO is

$$(5.2) \quad \Psi_{\text{ABO}}^h = \Psi_{\text{O}}^h \circ \Psi_{\text{B}}^h \circ \Psi_{\text{A}}^h$$

where $\Psi_{\text{A}}^h = (q + hp, 0)$, $\Psi_{\text{B}}^h = (q, p - h\nabla V(q))$ and for the O step we use the map

$$\Psi_{\text{O}}^h(q, p) = \left(q, \exp(-h\gamma)p + \sqrt{\beta^{-1}(1 - \exp(-2\gamma h))}R \right)$$

where $R \sim \mathcal{N}(0, 1)$. In the case of symmetric composition methods such as ABOBA, OBABO, etc., we view each of the A and B operations as being performed with a half time step. Each component can be identified with an associated generator \mathcal{L}_{A} , \mathcal{L}_{B} , and \mathcal{L}_{O} , where e.g.

$$\Psi_{\text{A}}^h \equiv \exp(h\mathcal{L}_{\text{A}}).$$

As in [21, 23] we write the discrete propagator in the form $\exp(t\mathcal{L})$ using a perturbation series

$$\hat{\mathcal{L}} = \mathcal{L}_{\text{LD}} + h\hat{\mathcal{L}}_1 + h^2\hat{\mathcal{L}}_2 + O(h^4),$$

and employ the Baker-Campbell-Hausdorff formula to work out the terms of the expansion [11]. The probability distribution associated to the discretization scheme can be assumed to have a density which evolves from timestep n to timestep $n+1$ by

$$\rho_{n+1} = \exp(h\hat{\mathcal{L}}^*)\rho_n,$$

where $\hat{\mathcal{L}}^*$ represents the L_2 -adjoint of $\hat{\mathcal{L}}$. In a similar way, BCH can be used to work out the terms of the adjoint of the generator. One useful property is that symmetric composition methods constructed in this way have even weak order, due to cancellation properties of the BCH expansion. In a typical case such symmetric schemes are found to be more efficient (greater accuracy per unit computational work) than their asymmetric counterparts, since we can often reuse a force evaluation performed at the end of one step at the start of the next. More details on the design and analysis of such splitting schemes may be found in [23].

Inspired by such splittings, we seek similar methods for the transformed system of SDEs (4.10) which requires the computation of extra terms such as $\nabla g(x)\beta^{-1}$, as well as rendering the step A implicit. If the correction term is included in Step B, we have

$$(5.3) \quad \hat{B} := \begin{cases} dx &= 0 \\ dp &= -\nabla V(x(t))g(x(t))dt + \nabla g(x)\beta^{-1}dt \end{cases},$$

$$(5.4) \quad \hat{O} := \begin{cases} dx &= 0 \\ dp &= -\gamma pg(x)dt + \sqrt{2\beta^{-1}g(x)}dW(t) \end{cases}.$$

Both of these vector fields can be evolved exactly, in the weak sense, with their solutions summarised in Algorithms 5.1 and 5.2.

Algorithm 5.1 A step of size h for \hat{B} . Inputs: X, P, h, G, G_p .

```

 $G \leftarrow g(X)$ 
 $F \leftarrow -\nabla V(X)$ 
 $G_p \leftarrow \nabla g(X)$ 
 $P \leftarrow P + h(GF + \beta^{-1}G_p)$ 
return  $P, G, F, G_p$ 

```

Algorithm 5.2 A step of size h for \hat{O} . Inputs: $X, P, h, G, g(x), -\nabla V(x), \nabla g(x)$.

```

 $G \leftarrow g(X)$ 
 $C \leftarrow \exp(-Gh\gamma)$ 
 $R \sim \mathcal{N}(0, 1)$ 
 $P \leftarrow CP + \sqrt{\beta^{-1}(1 - C^2)}R$ 
return  $P, G$ 

```

If we compute the correction term in step O we have

$$(5.5) \quad \tilde{B} := \begin{cases} dx &= 0 \\ dp &= -\nabla V(x(t))g(x(t))dt \end{cases},$$

$$(5.6) \quad \tilde{O} := \begin{cases} dx &= 0 \\ dp &= -\gamma pg(x)dt + \nabla g(x)\beta^{-1}dt + \sqrt{2\beta^{-1}\gamma g(x)}dW(t) \end{cases}.$$

Similarly, the step B step can be resolved using the Euler method while the steps O may be solved exactly as well, as these are OU process and the correction term only depends on x which is constant. For an OU process $dx = \theta(\mu - x_t)dt + \sigma dW_t$, the

drift terms are $\theta = \gamma g(x)$ and $\mu = \frac{\nabla g \beta^{-1}}{\gamma g(x)}$. The solution has mean $p_0 \exp(-\gamma g(x)dt) + \frac{\nabla g \beta^{-1}}{\gamma g} (1 - \exp(-\gamma g(x)dt))$ and variance $\sigma^2 = \frac{1}{\beta} (1 - \exp(-2\gamma g(x)dt))$. We summarize in Algorithms 5.3 and 5.4.

Algorithm 5.3 A step of size h for \tilde{B} . Inputs: $X, P, h, G, g(x), -\nabla V(x), \nabla g(x)$.

$F = -\nabla V(X)$
 $G = g(X)$
 $G_p = \nabla g(X)$
 $P := P + hGF$
return P, F, G, G_p

Algorithm 5.4 A step of size h for \tilde{O} . Inputs: X, P, h, G, G_p .

$G \leftarrow g(X)$
 $C \leftarrow \exp(-Gh\gamma)$
 $R \sim \mathcal{N}(0, 1)$
 $P := CP + \frac{G_p(1-C)}{\beta\gamma G} + \sqrt{\beta^{-1}(1-C^2)}R$
return P, G

For step A, the integration is a little more complicated. Due to the introduction of the monitor function g , the vector field becomes

$$(5.7) \quad \hat{A} := \begin{cases} dx &= pg(x)dt \\ dp &= 0 \end{cases}.$$

To obtain second order schemes, we need to discretize this ODE system by an appropriate method. We elect to use the implicit midpoint method and to solve the implicit equations by fixed point iteration. We write this as a step of length h , as follows:

$$(5.8) \quad x_{n+1} = x_n + hp_n g(x_{n+1/2})$$

where $x_{n+1/2} = \frac{x_n + x_{n+1}}{2}$. By adding x_n , multiplying by a factor two and applying the monitor function to both sides and writing $g_{n+1/2} = g(x_{n+1/2})$, we have

$$(5.9) \quad g_{n+1/2} = g(x_n + \frac{h}{2}pg_{n+1/2}).$$

The fixed point iteration is computed by

$$(5.10) \quad g_{n+1/2}^j = g(x_n + \frac{h}{2}pg_{n+1/2}^{j-1}),$$

with $j = 1, \dots, J$ and $g_n^0 = g(x_n)$, so that we obtain $x_{n+1} = x_n + hp_n g_{n+1/2}^J$. In practice we set a tolerance and a maximum number of iterations, however in general the scheme converges with $J = 5$. In the sequel we denote the various algorithms by $\hat{A}(h), \tilde{A}(h), \hat{B}(h), \tilde{B}(h), \hat{O}(h), \tilde{O}(h)$, where, among the inputs, just the stepsize is explicitly indicated. We thus obtain two schemes by composition:

$$\hat{\Psi}_h = \hat{B}(h/2)\hat{A}(h/2)\hat{O}(h)\hat{A}(h/2)\hat{B}(h/2)$$

$$\tilde{\Psi}_h = \tilde{B}(h/2)\tilde{A}(h/2)\tilde{O}(h)\tilde{A}(h/2)\tilde{B}(h/2).$$

Each of these methods requires at least four evaluations of the monitor function g and two of the function g' , and these evaluations are potentially more computationally intensive for step A, depending on the number of iterations needed. We make the working assumption that the function $g : \mathbb{R} \rightarrow \mathbb{R}$ can be constructed based on a greatly simplified expression compared to the full computation of the potential energy function, so we anticipate that the added computational cost is relatively small in large dimensional settings.

6. Numerical experiments. After reviewing the properties of the discretization schemes applied to the IP transformed SDEs (2.13) and (4.10), we describe numerical simulations to illustrate the results. The examples illustrate that computational effort can be reduced while obtaining a similar accuracy. We compute functional of the processes to evaluate the weak error. The error in the sampled distribution $\hat{\rho}$ is reduced to an average of an observable ϕ at time $t > 0$ [24], the true value $\bar{\phi}$ is computed analytically or by quadrature via *scipy.integrate.quad* [48]. The observable estimated by a numerical timestepping scheme with step h is $\hat{\phi}(t, h)$. We have

$$\begin{aligned}\bar{\phi}(t) &= E_{\rho(t, \cdot)}\phi = \int_{\mathbb{R}^d} \phi(x)\rho(t, x)dx, \\ \hat{\phi}(t, h) &= E_{\rho_N(\cdot)}\phi = \frac{1}{M} \sum_{i=1}^{n_s} \phi(X_i^N),\end{aligned}$$

where the sample i approximates $X_i^N \approx x(t = hn_s)$, and a large number of trajectories are computed to reduce the sampling error. A time-discrete approximation converges weakly with order $r > 0$ at time T if there exists a positive constant C which does not depend on the stepsize h such that $|\hat{\phi}(t) - \bar{\phi}(t, h)| \leq Ch^r$ [19, chapter 9, section 6]. A good observable captures most of the behaviour of the distribution of interest. We choose the observable as the moments up to order $k \in \mathbb{N}_0$ such that $\phi(x) = x^k$ as in [19, Chapter 9, Section 4].

6.1. Square potential with sudden change of steepness.

6.1.1. Overdamped transformed dynamic. The example is presented in Section 2, with the potential given by (2.2), plotted in Figure 1(a), the choice of monitor function is given by (3.1) with $g_3(x) = \psi(\omega(x))$. In Figure 6, the order of convergence is similar for both the Euler-Maruyama applied to the transformed Langevin and the Langevin dynamic. The asymptotic regime is reached for a larger stepsize for the transformed overdamped dynamic, while the overdamped has not reached its asymptotic regime for this stepsize. This gain in efficiency for the transformed dynamic is not due to a smaller average step, as the average value taken by the monitor function is 1.18. It implies that a larger average steps yields better results. This shows a gain in efficiency.

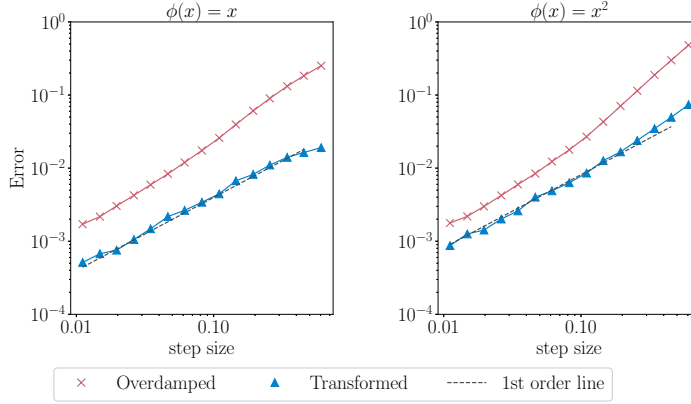


FIG. 6. *Order of Accuracy in the case of the squarred potential with change of steepness with final time $T = 100$ and stepsize between 0.3 and 1.48 with a mean of 1.2, number of trajectories is $n_s = 10^8$, $M = 1.5$, $m = 0.001$, $\tau = 0.1$ ($a = 2.75$, $b = 0.1$, $c = 0.1$, $x_0 = 0.5$)*

To prove that there are no changes in the order of convergence of the method, a similar simulation is ran but with parameters that renders the potential less steep, and thus easier to integrate. In Figure 7, the order of convergence of the Euler-Maruyama method is recovered for larger stepsize for both dynamics. This is due to the potential being easier to integrate. It is close to an harmonic potential. The smaller error arising in the transformed case is this time due simply to the smaller average steps the method take, 0.77. The example is very easy to numerically integrate and no benefits can be gained from the transformed dynamics.

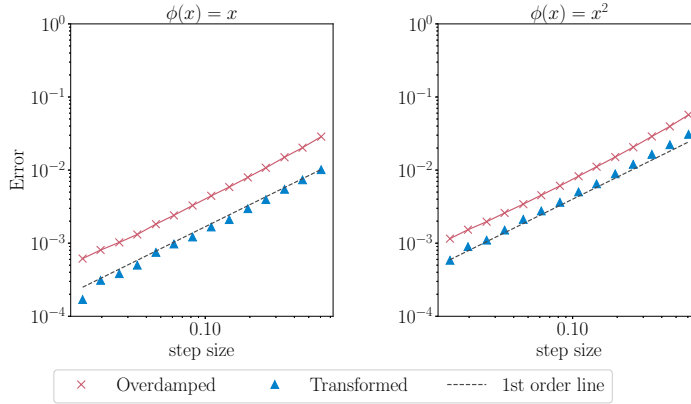


FIG. 7. *Order of Accuracy in the case of squarred potential with change of steepness with final time $T = 100$ and stepsize between 0.6 and 1.37 with a mean of 0.77, number of trajectories is $n_s = 10^8$, $M = 1.5$, $m = 0.001$, $\tau = 0.1$ ($a = 1$, $b = 1$, $c = 0.1$, $x_0 = 0.5$)*

6.1.2. Underdamped transformed dynamic. In this section, we introduce the results comparing the results obtained on the BAOAB scheme applied to the system (1.1) and the discretization methods developed in Section 5, BAOAB and BAOAB, applied to the example set in Section 2, with the potential given by (2.2)

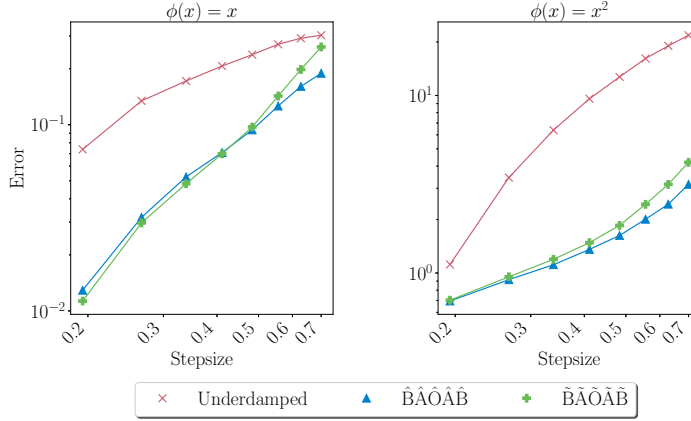


FIG. 8. *Observable in the case of squared potential with change of steepness with final time $T = 100$ and stepsize between 0.1 and 0.7, number of trajectories is $n_s = 10^8$, $M = 1.3$, $m = 0.001$, $\tau = 0.1$ and $\gamma = 0.1$ ($a = 15$, $b = 0.1$, $c = 0.1, x_0 = 0.5$)*

We can make the problem more difficult by setting $a = 4$, which is more difficult to numerically integrate and we obtain the figure 9.

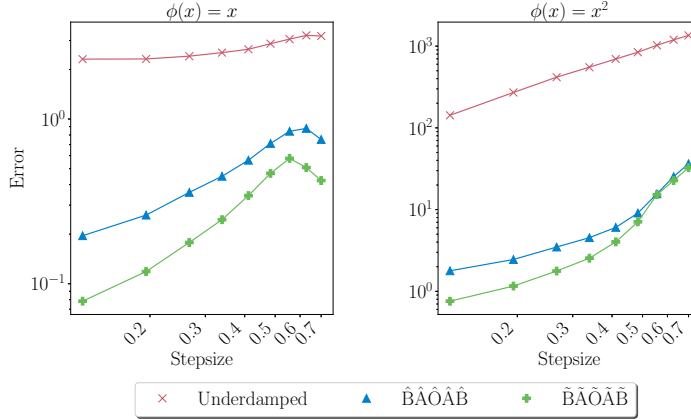


FIG. 9. *Observables in the case of squared potential with change of steepness with final time $T = 100$ and stepsize between 0.1 and 2.014, number of trajectories is $n_s = 5 \cdot 10^8$, $M = 1.3$, $m = 0.001$, $\tau = 0.1$ and $\gamma = 0.1$ ($a = 15$, $b = 0.1$, $c = 0.1, x_0 = 0.5$)*

We can note that when the algorithm $\hat{B}\hat{A}\hat{O}\hat{A}\hat{B}$ is used, the error is slightly larger than when the algorithm $\hat{B}\hat{A}\hat{O}\hat{A}\hat{B}$ is used. This is due to the fact that the numerical implementation solving the correction in step O is exact. In addition, we observe that the adaptive algorithms present an advantage at large stepsize. They provide a reasonable approximation of the distribution for relatively large stepsize. The main advantage of this method resides in the fact that the asymptotic behaviour is reached for relatively larger stepsize.

6.2. A Bayesian example. Bayesian inference [9] often requires sampling algorithms to approximate so-called posterior distributions. When the Bayesian frame-

work is used to represent variables on bounded sets, e.g., in the training of deep learning [25] or otherwise [47], Langevin-based sampling algorithms are difficult to apply. Hard bounds need to be encoded with boundary conditions, softer bounds produce large gradients in the potential close to the boundary. We now consider such an inference problem, where we observe data $y_1, \dots, y_N \sim \mathcal{N}(\mu, 1)$ i.i.d. with an unknown $\mu \in \mathbb{R}$. A priori, we know that the true value of μ lies in the interval $[1, 3]$, which we enforce through a prior distribution that is smoothly bounded. We aim to sample from the posterior distribution ρ_{Bayes} in this setting given by

$$\rho_{\text{Bayes}}(\mu) \propto \prod_{i=1}^N \exp\left(-\frac{\|y_i - \mu\|^2}{2}\right) \exp\left(-(\mu - a)^{2K}\right)$$

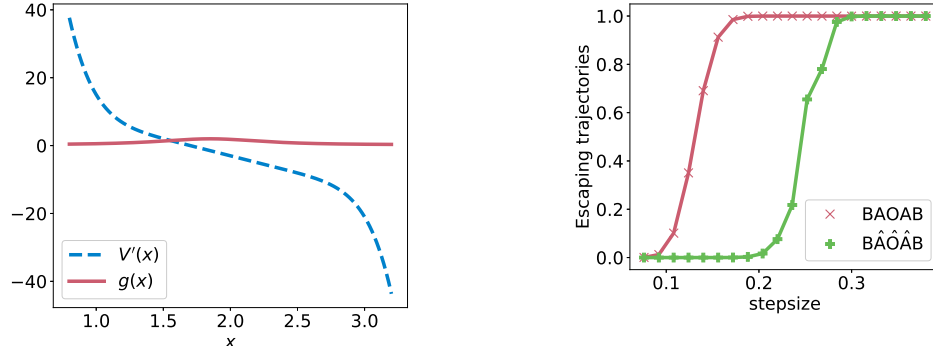
where the parameters K controls the steepness of the bounds in the approximately uniform prior. To stay in the same setting, as before, we aim at sampling from the potential $V(\mu) = \log p(\mu|\mathbf{x})\pi(\mu)$ such that

$$V'(\mu) = -\left(\sum_{i=1}^N y_i - N\mu - 2K(\mu - a)^{2K-1}\right).$$

An adaptive function adjusted to the prior and the likelihood is for instance

$$g(\mu) = \psi\left(r\left(\mu - a + 0.5\left(\frac{\sum_{i=1}^N y_i}{N} - a\right)^2\right)\right)$$

where the parameter r adjust the adaptivity of the monitor function. The parameters used are $K = 4$, $a = 2$, $r = 2$, $\tau = 0.1$, $\gamma = 0.1$ and $m = 0.1$ and $M = 1$. The data are simulated using $y_i \sim \mathcal{N}(1.7, 1)$ with $N = 10$. The average step in the BAOAB algorithm is adjusted to the average value of the monitor function in the $\tilde{\text{BAOAB}}$ algorithm.



(a) The gradient V' and an example of monitor function g

(b) The percentage of escaping trajectories over 10^5 runs with the two different algorithms until $T = 10^5$.

FIG. 10. Plots for the Bayesian example and proportion of trajectories that are unstable for different stepsizes.

In Fig 10(b), the adaptive algorithm yield less escaping trajectories for a similar stepsize. The stepsize used in BAOAB is rescaled by the smallest average value taken

by the monitor function g over the simulations in $\tilde{\text{BA}}\tilde{\text{O}}\tilde{\text{A}}\tilde{\text{B}}$, i.e. 0.85. This means that the adaptive algorithm is more stable as it yields less unstable trajectories. This shows that the adaptive methods allows us to use larger stepsizes and save computational effort. Indeed, in Figure 11, one can see that using a larger stepsize $h = 0.191$ with the BAOAB algorithm leads to poor sampling. This is due to the large proportion of trajectories that are unstable and are excluded from the histogram. Comparatively, the method $\tilde{\text{BA}}\tilde{\text{O}}\tilde{\text{A}}\tilde{\text{B}}$ allows us to obtain a good sample of the invariant distribution. With the small stepsize $h = 0.01$, both methods sample accurately the invariant distribution.

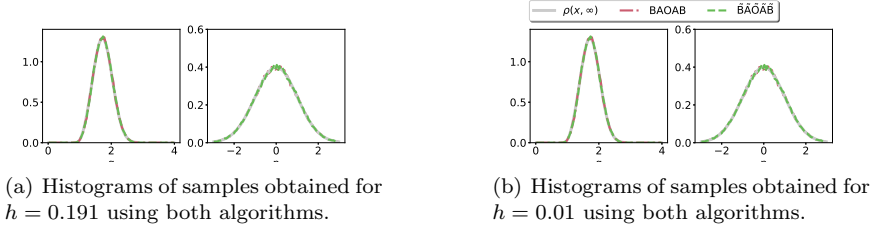


FIG. 11. Histograms of the samples obtained for the different algorithms for different stepsizes.

6.3. Example 2D: a system with two pathways. We next turn to a more complicated example. This system is still planar but we now introduce two channels: one narrow valley in the energy landscape and a second, set at a slightly higher energy level, is much wider and shallower, and is thus entropically favored at modest temperature. The energy function is

$$(6.1) \quad q(x, y) = \frac{1 + k_1 p_1(x, y) p_2(x, y)}{1 + p_1(x, y)} + k_3 \frac{k_2 p_1(x, y) p_2(x, y)}{1 + k_2 p_2(x, y)} + k_4 x^2$$

where $p_1(x, y) = (y - x^2 + 4)^2$ and $p_2(x, y) = (y + x^2 - 4)^2$. In our experiments we set $k_1 = 0.1$, $k_2 = 50$, $k_3 = 50$, $k_4 = 0.1$. The parameters can be tuned to influence how difficult is the potential we aim at integrating. The dynamics of this system unfold in the vicinity of two parabolic arcs, with the contour plot of the potential shown in Fig. 12(a). We begin by solving the problem using a fixed-stepsize Langevin integrator with a small stepsize, results are shown in Figure 12(b).

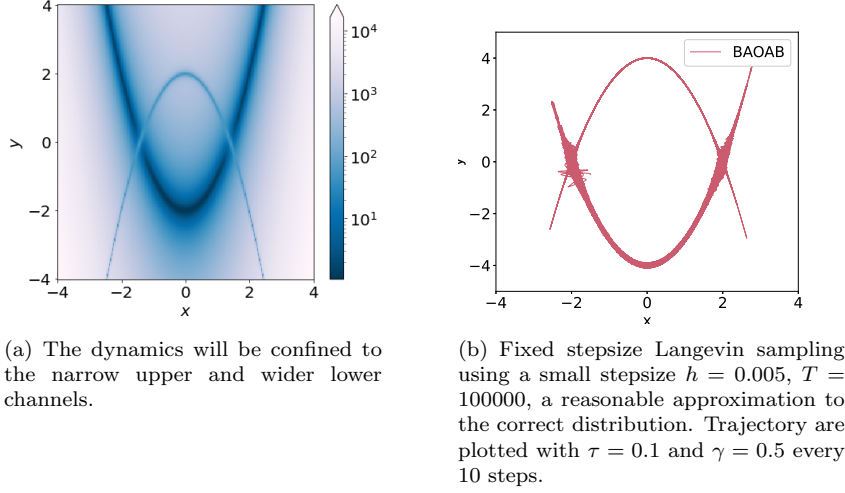


FIG. 12. *The two-path problem with both wide and narrow valleys.*

This simulation is reproduced using a larger stepsize ($h = 0.025$) alongside the results of the adaptive algorithms $\tilde{\text{BAOAB}}$. The results, shown in Fig. 12 show that the sampling of the target distribution is poor. The obvious cause is the large stepsize as we can in right hand panel frequent failed attempts to enter the narrow channel.

For this purpose, we design a monitor function that reduces the stepsize when close to the upper narrow channel. We use the design presented in equation (3.1) such that

$$\begin{aligned}\tilde{g}(x, y) &:= g(f(x, y)) \\ f(x, y) &= (y + x^2 - 4)^2\end{aligned}$$

with $m = 0.2$ and $M = 1$. In the results presented in Figure 13, we have adjusted the size of the step in the $\tilde{\text{BAOAB}}$ method to match the average value taken by the monitor function g over the entire trajectory, in that way we provide a comparison for a similar computational effort. The average value taken by the monitor function is 0.65.

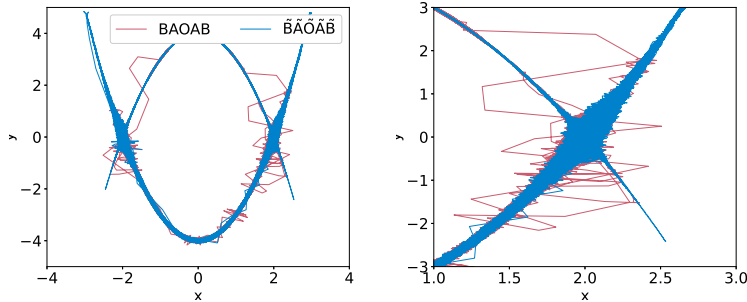


FIG. 13. *Plots of the trajectories with the classic underdamped system and the transformed underdamped system. The stepsize is $h = 0.025$, rescaled by the average value of the monitor function 0.741 for the classic underdamped. The transformed system is able to visit the upper narrow channel while the classic system can not.*

Note integrating the narrower parts of the lower wider channel is difficult for the transformed stepsize as the monitor function only reduces the step in the narrow upper channel and not at the extremities of the lower wider channel.

7. Conclusions. In this work, we have explored stochastic differential equations that are able to efficiently approximate a target probability distribution. These invariant-preserving transformed dynamics are fundamentally based on an adaptive time stepping in overdamped and underdamped Langevin dynamics, respectively. The target measure is preserved by adding a correction term to the usual, direct time-rescaled dynamics. Throughout this work, the adaptivity is controlled by a monitor function g , for the choice of which we provide both formal criteria and heuristics for applicants. The formal criteria ensure existence and uniqueness of weak solutions to the overdamped and underdamped IP transformed dynamics, as well as uniqueness of their invariant measure and ergodicity. The heuristics help users to design an appropriate monitor function that ensures efficiency. While numerical integration of the overdamped case is simple, we provide two novel splitting schemes to integrate the invariant-preserving transformed underdamped system. We illustrate the efficiency of these splitting schemes, as well as the efficiency of overdamped IP transformed discretised with Euler—Maruyama, in several examples.

REFERENCES

- [1] Y. BAO, M. RACHH, E. KEAVENY, L. GREENGARD, AND A. DONEV, *A fluctuating boundary integral method for brownian suspensions*, Journal of Computational Physics, 374 (2018), pp. 1094–1119, <https://doi.org/10.1016/j.jcp.2018.08.021>.
- [2] D. A. BEARD AND T. SCHLICK, *Inertial stochastic dynamics. I. Long-time-step methods for Langevin dynamics*, The Journal of Chemical Physics, 112 (2000), pp. 7313–7322, <https://doi.org/10.1063/1.481331>, <https://doi.org/10.1063/1.481331>, <https://arxiv.org/abs/https://pubs.aip.org/aip/jcp/article-pdf/112/17/7313/10806459/7313.1.online.pdf>.
- [3] M. BETANCOURT, *A conceptual introduction to hamiltonian monte carlo*, 2018, <https://arxiv.org/abs/1701.02434>.
- [4] N. BOU-RABEE AND H. OWHADI, *Long-run accuracy of variational integrators in the stochastic context*, SIAM journal on numerical analysis, 48 (2010), pp. 278–297.
- [5] P. BURRAGE AND K. BURRAGE, *A variable stepsize implementation for stochastic differential equations*, Journal of Scientific Computing, 24 (2002), pp. 848–864.
- [6] S. DUANE, A. KENNEDY, B. J. PENDLETON, AND D. ROWETH, *Hybrid monte carlo*, Physics Letters B, 195 (1987), pp. 216–222, [https://doi.org/https://doi.org/10.1016/0370-2693\(87\)91197-X](https://doi.org/https://doi.org/10.1016/0370-2693(87)91197-X), <https://www.sciencedirect.com/science/article/pii/037026938791197X>.
- [7] A. B. DUNCAN, T. LELIEVRE, AND G. A. PAVLIOTIS, *Variance reduction using nonreversible langevin samplers*, Journal of Statistical Physics, 163 (2016), pp. 457–491, <https://doi.org/10.1007/s10955-016-1491-2>, <https://doi.org/10.1007/s10955-016-1491-2>.
- [8] J. GAINES AND J. LYONS, *Variable step size control in the numerical solution of stochastic differential equations*, SIAM Journal on Applied Mathematics, 57 (1997), pp. 1455–1484.
- [9] D. GAMERMAN AND H. F. LOPES, *Markov chain Monte Carlo : stochastic simulation for Bayesian inference / Dani Gamerman, Hedibert Freitas Lopes.*, Texts in statistical science ; v. 68, Chapman & Hall, Boca Raton ;, second edition. ed., 2006.
- [10] M. GIROLAMI AND B. CALDERHEAD, *Riemann manifold langevin and hamiltonian monte carlo methods*, Journal of the Royal Statistical Society: Series B (Statistical Methodology), 73 (2011), pp. 123–214.
- [11] E. HAIRER, C. LUBICH, AND G. WANNER, *Geometric Numerical Integration: Structure-Preserving Algorithms for Ordinary Differential Equations*, vol. 31 of Springer series in computational mathematics, Springer Berlin / Heidelberg, Berlin, Heidelberg, 2 ed., 2006.
- [12] M. HAN, J. PARK, T. LEE, AND J. H. HAN, *Fluctuation-dissipation-type theorem in stochastic linear learning*, Phys. Rev. E, 104 (2021), p. 034126, <https://doi.org/10.1103/PhysRevE.104.034126>, <https://link.aps.org/doi/10.1103/PhysRevE.104.034126>.
- [13] L. HORMANDER, *Hypoelliptic second order differential equations*, Acta mathematica, 119 (1967), pp. 147–171.

- [14] W. HUANG AND B. LEIMKUHLE, *The adaptive Verlet method*, SIAM journal of computing scientific, 43 (1997), pp. 239–256.
- [15] W. HUANG, Y. REN, AND R. D. RUSSELL, *Moving mesh partial differential equations (mmpdes) based on the equidistribution principle*, SIAM Journal on Numerical Analysis, 31 (1994), pp. 709–730, <https://doi.org/10.1137/0731038>, <https://doi.org/10.1137/0731038>, <https://arxiv.org/abs/https://doi.org/10.1137/0731038>.
- [16] M. HÜTTER AND H. CHRISTIAN ÖTTINGER, *Fluctuation-dissipation theorem, kinetic stochastic integral and efficient simulations*, J. Chem. Soc., Faraday Trans., 94 (1998), pp. 1403–1405, <https://doi.org/10.1039/A800422F>, <http://dx.doi.org/10.1039/A800422F>.
- [17] N. KANTAS, P. PARPAS, AND G. A. PAVLIOTIS, *The sharp, the flat and the shallow: Can weakly interacting agents learn to escape bad minima?*, 2019, <https://arxiv.org/abs/1905.04121>.
- [18] C. KELLY AND G. J. LORD, *Adaptive timestepping strategies for nonlinear stochastic systems*, IMA J. Numer. Anal., 38 (2017), p. 1523–1549.
- [19] P. KLOEDEN AND E. PLATEN, *Numerical Solution of Stochastic Differential Equations*, Preprints aus dem Institut für Mathematik, Springer, 1999.
- [20] H. LAMBA AND A. MATTINGLY, J. AND STUART, *An adaptive Euler-Maruyama scheme for SDEs: convergence and stability*, IMA J. Numerical Analysis, 27 (2007).
- [21] B. LEIMKUHLE AND C. MATTHEWS, *Rational Construction of Stochastic Numerical Methods for Molecular Sampling*, Applied Mathematics Research eXpress, 2013 (2012), pp. 34–56, <https://doi.org/10.1093/amrx/abs010>, <https://doi.org/10.1093/amrx/abs010>, <https://arxiv.org/abs/https://academic.oup.com/amrx/article-pdf/2013/1/34/397230/abs010.pdf>.
- [22] B. LEIMKUHLE AND C. MATTHEWS, *Molecular Dynamics: With Deterministic and Stochastic Numerical Methods*, Interdisciplinary Applied Mathematics, Springer International Publishing, 2015.
- [23] B. LEIMKUHLE, C. MATTHEWS, AND G. STOLTZ, *The computation of averages from equilibrium and nonequilibrium langevin molecular dynamics*, IMA Journal of Numerical Analysis, 36 (2013), <https://doi.org/10.1093/imanum/dru056>.
- [24] B. LEIMKUHLE, C. MATTHEWS, AND M. TRETYAKOV, *On the long-time integration of stochastic gradient systems*, Proceedings of the Royal Society A: Mathematical, Physical and Engineering Sciences, 470 (2014), <https://doi.org/https://doi.org/10.1098/rspa.2014.0120>.
- [25] B. J. LEIMKUHLE, T. J. VLAAR, T. POUCHON, AND A. J. STORKEY, *Better training using weight-constrained stochastic dynamics*, in International Conference on Machine Learning, 2021, <https://api.semanticscholar.org/CorpusID:235490648>.
- [26] T. LELIEVRE, F. NIER, AND G. A. PAVLIOTIS, *Optimal non-reversible linear drift for the convergence to equilibrium of a diffusion*, Journal of Statistical Physics, 152 (2013), pp. 237–274, <https://doi.org/10.1007/s10955-013-0769-x>, <https://doi.org/10.1007/s10955-013-0769-x>.
- [27] T. LELIEVRE, M. ROUSSET, AND G. STOLTZ, *Free Energy Computations: A Mathematical Perspective*, Imperial College Press, 06 2010, <https://doi.org/10.1142/P579>.
- [28] T. LELIEVRE AND G. STOLTZ, *Partial differential equations and stochastic methods in molecular dynamics*, Acta Numerica, 25 (2016), p. 681–880, <https://doi.org/10.1017/S0962492916000039>.
- [29] V. LEMAIRE, *An adaptive scheme for the approximation of dissipative systems*, Stochastic Processes and their Applications, 117 (2007), pp. 1491–1518, <https://doi.org/https://doi.org/10.1016/j.spa.2007.02.004>, <https://www.sciencedirect.com/science/article/pii/S0304414907000233>.
- [30] Y.-A. MA, T. CHEN, AND E. B. FOX, *A complete recipe for stochastic gradient mcmc*, 2015, <https://arxiv.org/abs/1506.04696>.
- [31] S. MANDT, M. HOFFMAN, AND D. BLEI, *A variational analysis of stochastic gradient algorithms*, Proceedings of The 33rd International Conference on Machine Learning,, 48 (2016), pp. 354–363.
- [32] X. MAO, *The truncated euler-maruyama method for stochastic differential equations*, Journal of Computational and Applied Mathematics, 290 (2015), pp. 370–384.
- [33] J. MARTIN, L. C. WILCOX, C. BURSTEDDE, AND O. GHATTAS, *A stochastic newton mcmc method for large-scale statistical inverse problems with application to seismic inversion*, SIAM Journal on Scientific Computing, 34 (2012), pp. A1460–A1487, <https://doi.org/10.1137/110845598>, <https://doi.org/10.1137/110845598>, <https://arxiv.org/abs/https://doi.org/10.1137/110845598>.
- [34] J. MATTINGLY, A. STUART, AND M. TRETYAKOV, *Convergence of numerical time-averaging and stationary measures via poisson equations*, SIAM Journal on Numerical Analysis, 48 (2010), pp. 552–577, <http://www.jstor.org/stable/41062649> (accessed 2023-11-14).

- [35] J. MATTINGLY, A. M. STUART, AND D. J. HIGHAM, *Ergodicity for sdes and approximations: Locally lipschitz vector fields and degenerate noise*, Stochastic Processes and their Applications, 101 (2002), pp. 185–232, [https://doi.org/10.1016/S0304-4149\(02\)00150-3](https://doi.org/10.1016/S0304-4149(02)00150-3), [https://doi.org/10.1016/S0304-4149\(02\)00150-3](https://doi.org/10.1016/S0304-4149(02)00150-3).
- [36] S. MAUTHNER, *Step size control in the numerical solution of stochastic differential equations*, Journal of Computational and Applied Mathematics, 100 (1998), pp. 93–109, [https://doi.org/https://doi.org/10.1016/S0377-0427\(98\)00139-3](https://doi.org/https://doi.org/10.1016/S0377-0427(98)00139-3), <https://www.sciencedirect.com/science/article/pii/S0377042798001393>.
- [37] S. MELCHIONNA, *Design of quasi-symplectic propagators for langevin dynamics*, arXiv.org, (2007).
- [38] G. MILSTEIN AND M. TRETYAKOV, *Computing ergodic limits for langevin equations*, Physica D: Nonlinear Phenomena, 229 (2007), pp. 81–95, <https://doi.org/https://doi.org/10.1016/j.physd.2007.03.011>, <https://www.sciencedirect.com/science/article/pii/S0167278907000723>.
- [39] G. PAVLIOTIS, *Stochastic Processes and Applications*, Texts in Applied Mathematics, Springer, 2014.
- [40] G. O. ROBERTS AND O. STRAMER, *Langevin diffusions and metropolis-hastings algorithms*, Methodology And Computing In Applied Probability, 4 (2002), pp. 337–357, <https://api.semanticscholar.org/CorpusID:118594177>.
- [41] G. O. ROBERTS AND R. L. TWEEDIE, *Exponential convergence of Langevin distributions and their discrete approximations*, Bernoulli, 2 (1996), pp. 341 – 363.
- [42] G. O. ROBERTS AND R. L. TWEEDIE, *Geometric convergence and central limit theorems for multidimensional hastings and metropolis algorithms*, Biometrika, 83 (1996), pp. 95–110, <http://www.jstor.org/stable/2337435> (accessed 2023-11-27).
- [43] A. RÖSSLER, *An adaptive discretization algorithm for the weak approximation of stochastic differential equations*, Proc. Appl. Math. Mech., 19 (2004), pp. 19–22.
- [44] R. D. SKEEL AND J. A. IZAGUIRRE, *An impulse integrator for langevin dynamics*, Molecular physics, 100 (2002), pp. 3885–3891.
- [45] A. SZEPESSY, R. TEMPONE, AND G. E. ZOURARIS, *Adaptive weak approximation of stochastic differential equations*, Comm. Pure Appl. Math., 54 (2001), pp. 1051–1070.
- [46] A. VALINEJAD AND S. MOHAMMAD HOSSEINI, *A variable step-size control algorithm for the weak approximation of stochastic differential equations*, Numerical Algorithms, 55 (2001), pp. 429–446.
- [47] H. L. VAN TREES AND K. L. BELL, *Bayesian Bounds for Parameter Estimation and Nonlinear Filtering Tracking*, John Wiley & Sons, 2007.
- [48] P. VIRTANEN, R. GOMMERS, T. E. OLIPHANT, M. HABERLAND, T. REDDY, D. COURNAPEAU, E. BUROVSKI, P. PETERSON, W. WECKESSER, J. BRIGHT, S. J. VAN DER WALT, M. BRETT, J. WILSON, K. J. MILLMAN, N. MAYOROV, A. R. J. NELSON, E. JONES, R. KERN, E. LARSON, C. J. CAREY, Í. POLAT, Y. FENG, E. W. MOORE, J. VANDERPLAS, D. LAXALDE, J. PERKTOLD, R. CIMRMAN, I. HENRIKSEN, E. A. QUINTERO, C. R. HARRIS, A. M. ARCHIBALD, A. H. RIBEIRO, F. PEDREGOSA, P. VAN MULBREGT, AND SCI-PY 1.0 CONTRIBUTORS, *SciPy 1.0: Fundamental Algorithms for Scientific Computing in Python*, Nature Methods, 17 (2020), pp. 261–272, <https://doi.org/10.1038/s41592-019-0686-2>.
- [49] B. K. ØKSENDAL, *Stochastic differential equations : an introduction with applications / Bernt Øksendal.*, Universitext, Springer, Berlin ;, sixth edition. ed., 2003.